Applied Surface Science 288 (2014) 430–434

Contents lists available at ScienceDirect

Applied Surface Science

journal homepage: www.elsevier.com/locate/apsusc

Atomic layer deposited Al_2O_3 films for anti-reflectance and surface passivation applications

Li Qiang Zhu*, Yang Hui Liu, Hong Liang Zhang, Hui Xiao, Li Qiang Guo

Ningbo Institute of Materials Technology and Engineering, Chinese Academy of Sciences, Ningbo 315201, People's Republic of China

ARTICLE INFO

Article history:
Received 25 August 2013
Received in revised form
24 September 2013
Accepted 9 October 2013
Available online 18 October 2013

Keywords:
Al2O3 films
Anti-reflectance
Surface passivation
X-ray photoelectron spectroscopy

ABSTRACT

Al_2O_3 films were deposited on n-type crystalline Si (c-Si) wafers by atomic layer deposition using $Al(CH_3)_3$ and H_2O as precursors. Surface anti-reflectance and passivation performances were investigated. Average reflectances between 2.8 and 4.2% were obtained for Al_2O_3 coated textured Si with Al_2O_3 thickness ranged between 100 and 70 nm. Wide thickness window for low reflectance between 2.8 and 4.2% indicates its potential anti-reflectance applications. A high minor carrier lifetime of ~4.5 ms is obtained for n-type c-Si wafers passivated by 100 nm Al_2O_3 films, corresponding to an effective surface recombination velocity of ~4 cm/s. Wide annealing time window and wide annealing temperature window are addressed to obtain good passivation performances with high minor carrier lifetime >3 ms. The passivation performances are related to the released H atoms from Al–OH bonds and the formation of Al vacancies and O interstitials within Al_2O_3 films. Our results indicate that Al_2O_3 films show dual functions of anti-reflectance and surface passivation for photovoltaic applications.

1. Introductions

It is reported that excellent surface passivation is essential for improving energy conversion efficiency in solar cells [1]. Recently, Al_2O_3 films have been received tremendous interests in photovoltaic communities [2–4]. Due to a high density of negative fixed charges (Q_{fix}) above 10^{12} cm^{-2} within Al_2O_3 layer, excellent field-effective passivation performances have been observed on both lightly and highly doped p- and n-type c-Si surfaces at a certain doping range [4–8]. Moreover, due to the high densities of negative fixed charges (Q_{fix}) and low densities of interface defects (D_{it}), the parasitic shunting effects are also overcome in p-type Si [9]. As the excellent surface passivation is essential to improve the efficiency, passivated emitter and rear locally diffused (PERL) or passivated emitter and rear cell (PERC) concepts with dual Si surface effectively passivated have been proposed[1,10,11]. A high efficiency of ~23.2% has been reported by passivating front side boron emitter with Al_2O_3 films for n-type PERL cell [10,11]. At the same time, effective anti-reflectance plays an important role for improving efficiency in solar cells. Conventionally, SiN_x layer is used as a front-side anti-reflective layer in c-Si solar cells [12]. Average reflectance is below 5%. It is reported that reflective index of Al_2O_3 films is ~1.65 at wavelength of 630 nm [13,14], suggesting its possibilities for anti-reflective applications in c-Si solar cells. Though, Al_2O_3 films with thickness below 50 nm have exhibited high passivation performances on c-Si surface; anti-reflective properties of Al_2O_3 films are needed to be discussed in detail. Moreover, studies on physical origins for passivation performances of Al_2O_3 films on c-Si surface are also interesting. In this paper, both anti-reflective properties and passivation performances of Al_2O_3 films deposited by atomic layer deposition (ALD) are studied. Though the deposition rate is not high in our case, a high deposition rate could be addressed by using high speed spatial atomic-layer deposition systems [15]. In this contribution, we focus on good anti-reflectance and passivation performances for the ALD deposited Al_2O_3 films. A wide thickness window for average reflectance between 2.8 and 4.2% is observed. A high minority carrier lifetime of ~4.5 ms is addressed. Physical origins for the passivation performances are discussed. The results here indicate that Al_2O_3 films have a dual function of surface passivation and anti-reflectance for potential photovoltaic applications.

2. Experimental detail

Phosphorous-doped n-type Czochralski (Cz) single crystalline Si (c-Si) wafers (Shiny-etched, (100)-oriented, 400 μm thick) were used as substrates. For anti-reflective studies, c-Si wafers were textured by NaOH solution. Then, the substrates underwent a dilute HCl solution dip followed by a dilute HF solution dip. A deionized water rinse was adopted after each chemical dip steps. Al_2O_3 films were deposited on the textured c-Si wafers in a thermal NCD 200B ALD reactor at 200 °C with a 100 sccm background flow of N_2.

* Corresponding author. Tel.: +86 574 86686791; fax: +86 574 86690355.
E-mail address: lqzhu@nimte.ac.cn (L.Q. Zhu).

0169-4332/$ – see front matter © 2013 Elsevier B.V. All rights reserved.
http://dx.doi.org/10.1016/j.apsusc.2013.10.051

$Al(CH_3)_3$ (TMA) and water (H_2O) were used as precursors. A cycle in the reactor consisted of two separate half-reactions. The first half-reaction was consisted of a 0.3 s injection of TMA vapor followed by 7 s N_2 purge. While the oxidation step was consisted of a 0.1 s injection of H_2O vapor followed by a 7 s N_2 purge. Al_2O_3 films were also deposited on shiny-etched Si wafers for measuring thickness and optical constants. Al_2O_3 films with thickness of 30, 45 and 60 nm were also deposited on 30 nm SiN_x coated textured Si for comparison. To study passivation performances, 100 nm thick Al_2O_3 films were deposited on both sides of shiny-etched c-Si wafers at the same condition. Post-deposition annealing (PDA) was performed in a quartz furnace at different temperature for different time under atmosphere ambient.

A cross-sectional morphology and top-view morphology were characterized by field-emission scanning electron microscopy (FE-SEM) for Al_2O_3 coated textured Si. SEM surface morphology characteristics were also performed for 100 nm Al_2O_3 passivated Si wafers (PDA at 350 °C for 10 min and at 450 °C for 2 min). No blistering was observed (results not shown here). Spectroscopic ellipsometry (SE) was used to obtain optical constants (n, k) and thickness of Al_2O_3 films. Reflectance spectra were obtained by using AudioDev's Helios LAB-rc system. Average reflectance was calculated with wavelength ranged between 380 and 1090 nm. Effective minority carrier lifetime (τ_{eff}) was obtained on a Semilab WT-2000PVN lifetime tester. The maximum effective surface recombination velocity S_{eff} could be calculated from τ_{eff} using the following equation [7]

$$S_{eff} = \frac{W}{2\tau_{eff}},$$

where W is the wafer thickness. Bulk minority carrier lifetime was assumed to be infinite. Accordingly, the calculated S_{eff} value marks an upper limit to the S_{eff}. X-ray photoelectron spectroscopy (XPS) measurements were carried out to study chemical bonds and chemical composition of Al_2O_3 films.

3. Results and discussions

3.1. Anti-reflectance performance

Anisotropic wet-chemical etching of c-Si in alkaline solution leads to the pyramidal surface topography. Fig. 1 (a) shows a scanning electron microscopy (SEM) image of surface morphology for Al_2O_3 coated textured Si surface. (111) oriented Si crystal planes remain at the surface forming the pyramids [16]. Fig. 1 (b) shows a SEM cross-sectional image of the Al_2O_3 coated textured Si wafer. Thickness of the textured surface is estimated to be ~3 μm. An Al_2O_3 layer is obviously observed to be covered on the pyramids with thickness of ~100 nm, consistent to the thickness obtained from spectroscopic ellipsometry. The textured surface helps to reduce optical average reflectance from ~29.4% before texturing to ~14.2% after texturing. Al_2O_3 over layer would reduce the average reflectance further, as will be discussed below.

Spectroscopic ellipsometry (SE) has been employed to investigate optical characteristics of Al_2O_3 films. Fig. 2 (a) illustrates the refractive index (n) and extinction coefficients (k) for as-deposited Al_2O_3 films with thickness of ~100 nm. Refractive index is measured to be ~1.65 at wavelength of 630 nm, similar to the reported value [13]. Fig. 2 (b) shows absorption coefficient (α) obtained by a relationship, $\alpha = 4\pi k/\lambda$, where λ is the wavelength of a photon. Optical band gap energy (E_g) is estimated to be ~6 eV with relation $\alpha h\nu \propto \left(h\nu - E_g\right)^2$, where $h\nu$ is photon energy [17]. Therefore, the deposited Al_2O_3 layer is transparent for photon with wavelength above ~200 nm. The obtained results suggest that Al_2O_3 films could be the potential anti-reflective layers in solar cells.

Fig. 3(a) shows the reflectance spectrum of Al_2O_3/SiN_x dual-layer coated textured Si wafers. The thickness of SiN_x layer is ~30 nm. It could be seen that the reflectance decreases with the increase of Al_2O_3 thickness (D). Fig. 3(b) shows the average reflectance (η) as a function of D. When there is no Al_2O_3 layer on 30 nm SiN_x, the average reflectance is ~13.4%. After depositing 30 and 45 nm Al_2O_3 on 30 nm SiN_x, the average reflectance decreases to ~8.9 and ~5.9%, respectively. The lowest reflectance of ~4.6% is obtained by depositing 60 nm Al_2O_3 on 30 nm SiN_x. Fig. 3(c) shows average reflectances (η) of Al_2O_3 coated textured Si wafers as a function of Al_2O_3 thickness (D). For the bare textured Si, a high average reflectance of ~14.2% is obtained. After depositing Al_2O_3 films with thickness of ~30 nm on the textured Si, average reflectance decreases to ~10.6%. With the increase of Al_2O_3 thickness, average reflectance decreases further. The lowest average reflectance of ~2.8% is obtained for Al_2O_3 films with thickness of ~100 nm on the textured Si. Fig. 3(d) shows the reflectance spectrum of textured Si, 100 nm Al_2O_3 coated textured Si and 74 nm SiN_x coated textured Si. At shorter wavelength, the reflectance for ~100 nm Al_2O_3 coated sample is a little higher than that for 74 nm SiN_x coated sample, while at longer wavelength, the reflectance for ~100 nm Al_2O_3 coated sample is a little lower than that for the 74 nm SiN_x coated sample. Such difference may be due to the different refractive index between SiN_x and Al_2O_3. Interestingly, a near linear relationship between average reflectance (η) and Al_2O_3 thickness (D) is obtained though the last two data deviate from the linear relationship, as shown in Fig. 3 (c). Average reflectance would decrease for ~0.12% when the thickness of Al_2O_3 films increase for 1 nm. Such linear relation is related to the optical path-length-dependent optical wave transport across the air/Al_2O_3/Si medium. For standard SiN_x (STD SiN_x) coated textured Si obtained from production line (Xinyou Photovoltaics Industry), average reflectance (η) is ranged between 2.5 and 5% with SiN_x thickness of ~70 ± 5 nm. The thickness window is ~10 nm to obtain the good anti-reflective performances for STD SiN_x. For Al_2O_3 coated textured Si wafers here, thickness of Al_2O_3 films is ranged between ~100 and ~70 nm with η ranged between 2.8 and 4.2%. Wide thickness window for

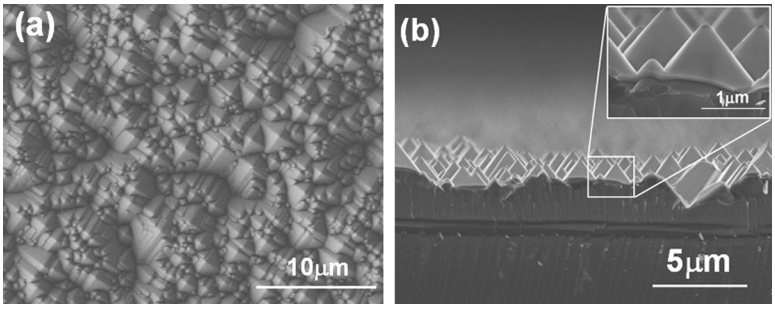

Fig. 1. (a) SEM top view images for 100 nm Al_2O_3 coated textured Si surface of a (100)-oriented c-Si wafer after anisotropical wet chemical etching leaving (111) planes. (b) SEM cross-sectional images of the 100 nm Al_2O_3 coated textured Si.

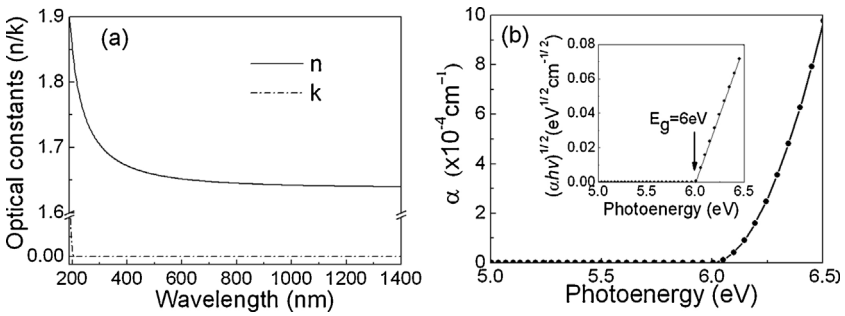

Fig. 2. (a) Optical constants (n, k) as a function of wavelength for as-deposited Al_2O_3 films with thickness of ~100 nm. (b) α vs $h\nu$ plot of as-deposited Al_2O_3 films. The inset figure shows $(\alpha h\nu)^{1/2}$ vs $h\nu$ plot. The intersection indicates the optical band gap energy (E_g) value.

low average reflectance suggests its potential anti-reflective applications for Al_2O_3 films in c-Si solar cells.

3.2. Passivation performances

For original n-type c-Si wafer, a low minority carrier lifetime (τ_{eff}) of ~13 μs is obtained, corresponding to an effective surface recombination velocity (S_{eff}) of ~1500 cm/s. After depositing 100 nm Al_2O_3 films, a higher τ_{eff} of ~1.2 ms is obtained, corresponding to a lower S_{eff} of ~17 cm/s. The results show that effective minor carrier lifetime is improved when Al_2O_3 films are deposited on c-Si surface. To study the full potential for surface passivation and thermal stability of the Al_2O_3 films, the lifetime samples were exposed to post-deposition annealing (PDA) under atmosphere ambient. Fig. 4 illustrates effective minority carrier lifetime (τ_{eff}) and surface recombination velocity (S_{eff}) of n-type c-Si wafers passivated by 100 nm Al_2O_3. Fig. 4 (a) illustrates post deposition annealing (PDA) temperature (T_a) dependent passivation performances with PDA time of 2 min. High level surface passivation performances with τ_{eff} > 3 ms and S_{eff} < 6 cm/s are obtained for T_a ranged between 350 and 550 °C. While for higher PDA temperature, the passivation performances degrade. The lifetime decreases to ~1.7 ms at 600 °C, corresponding to S_{eff} of ~12 cm/s. The results here indicate the wide annealing temperature window for obtaining good passivation performances.

Annealing time dependent passivation performances are also studied for PDA temperature at 350 °C. Fig. 4 (b) illustrates minority carrier lifetime (τ_{eff}) as a function of PDA time at T_a = 350 °C. For short annealing time of 30 s, a relative small lifetime below 2 ms is obtained, corresponding to a relatively high S_{eff} above 10 cm/s. While for annealing time ranged between 1 and 5 min, a high lifetime ranged between 3.5 and 4.5 ms is obtained, corresponding to lower S_{eff} ranged between 5.5 and 4.5 cm/s. With the increased annealing time above 6 min, the lifetime decreases to below 2.5 ms, corresponding to S_{eff} above 8 cm/s. Though such degradation, the lifetime is still above 1 ms, and the S_{eff} is still below 20 cm/s. The results here indicate the wide annealing time window for obtaining good passivation performances.

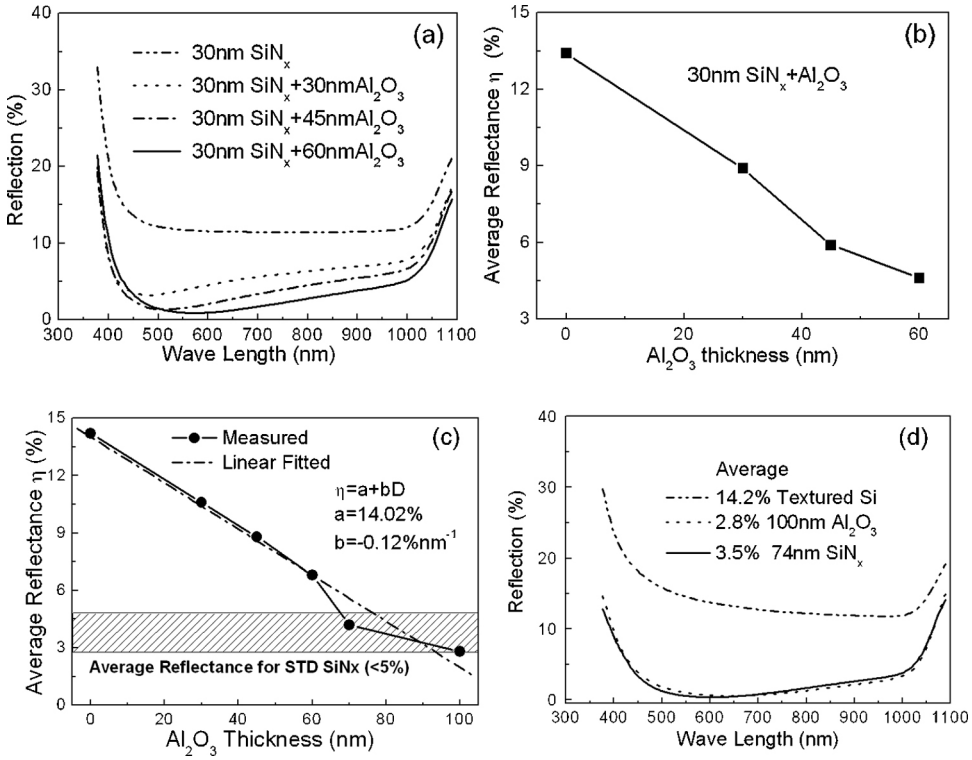

Fig. 3. (a) Reflectance spectrum of Al_2O_3/SiN_x dual-layer coated textured Si wafers. Thickness of SiN_x layer is ~30 nm. Al_2O_3 thickness (D) is ranged between 0 and 60 nm. (b) Average reflectance (η) of Al_2O_3/SiN_x dual-layer coated textured Si wafers as a function of D. (c) Average reflectance (η) for Al_2O_3 coated textured Si wafers as a function of D. A near linear relation is observed between η and D. (d) Reflectance spectrum of textured Si, 100 nm Al_2O_3 coated textured Si and 74 nm SiN_x coated textured Si.

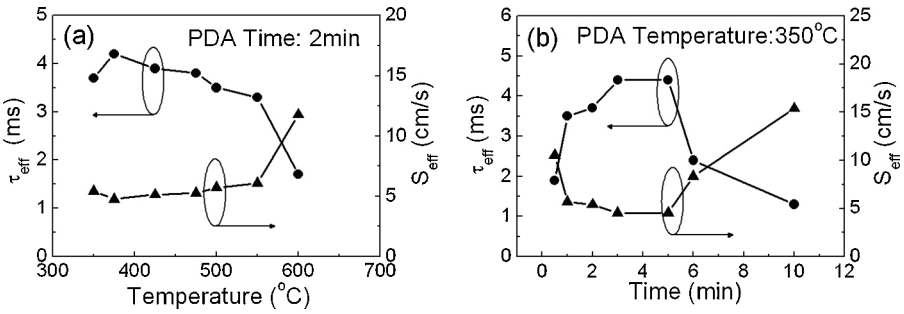

Fig. 4. Effective minority carrier lifetime (τ_{eff}) and effective surface recombination velocity (S_{eff}) of n-type c-Si wafers passivated by 100 nm thick Al_2O_3. (a) PDA temperature (T_a) dependent passivation performances with PDA time of 2 min. (b) PDA time dependent passivation performances with PDA temperature of 350 °C.

XPS measurements were performed to study passivation mechanisms. The wide-survey scan X-ray photoelectron spectra for as-deposited Al_2O_3 films and 550 °C annealed Al_2O_3 films are shown in Fig. 5 (a). A series of peaks from Al_{2p}, Al_{2s}, C_{1s}, and O_{1s} are clearly observed. The C_{1s} peak at binding energy of ~285.0 eV arises from the presence of hydrocarbon species at surface contamination [18]. Fig. 5 (b) shows Al_{2p} core-level XPS spectra. For as-deposited Al_2O_3 films, two components are observed at binding energies of 74.6 and 76.6 eV, corresponding to O–Al–O bonds and Al–OH bonds, respectively. After PDA annealing, the component at 76.6 eV disappears, while the peak at binding energy of ~74.6 eV remains, indicating the disappearance of Al–OH bonds during PDA process. Fig. 5 (c) shows O_{1s} core-level XPS spectra. For as-deposited Al_2O_3 films, two components are observed at binding energies of 531.6 and 532.8 eV, corresponding to Al–O–Al bonds and Al–OH bonds, respectively. After PDA annealing, the component at 532.8 eV disappears, indicating the disappearance of Al–OH bonds within the Al_2O_3 films. Peacock and Robertson indicated that interstitial H in Al_2O_3 would act as a deep trap site for electrons [19]. It should be noted here that some residual Al–OH bonds are produced during ALD reaction between TMA and H_2O. During PDA process, the residual O–H bonds would be broken easily, resulting in the interstitial H atoms within Al_2O_3 matrix. Such interstitial H atoms play an important role in passivation performances. Firstly, such H atoms would act as deep trap sites for electrons. Secondly, the released H atoms would also arrive at Al_2O_3/Si interface and passivate dangling bonds at Si surface. At the same time, PDA annealing promotes the formation of Al vacancies and O interstitials within Al_2O_3 films, which also

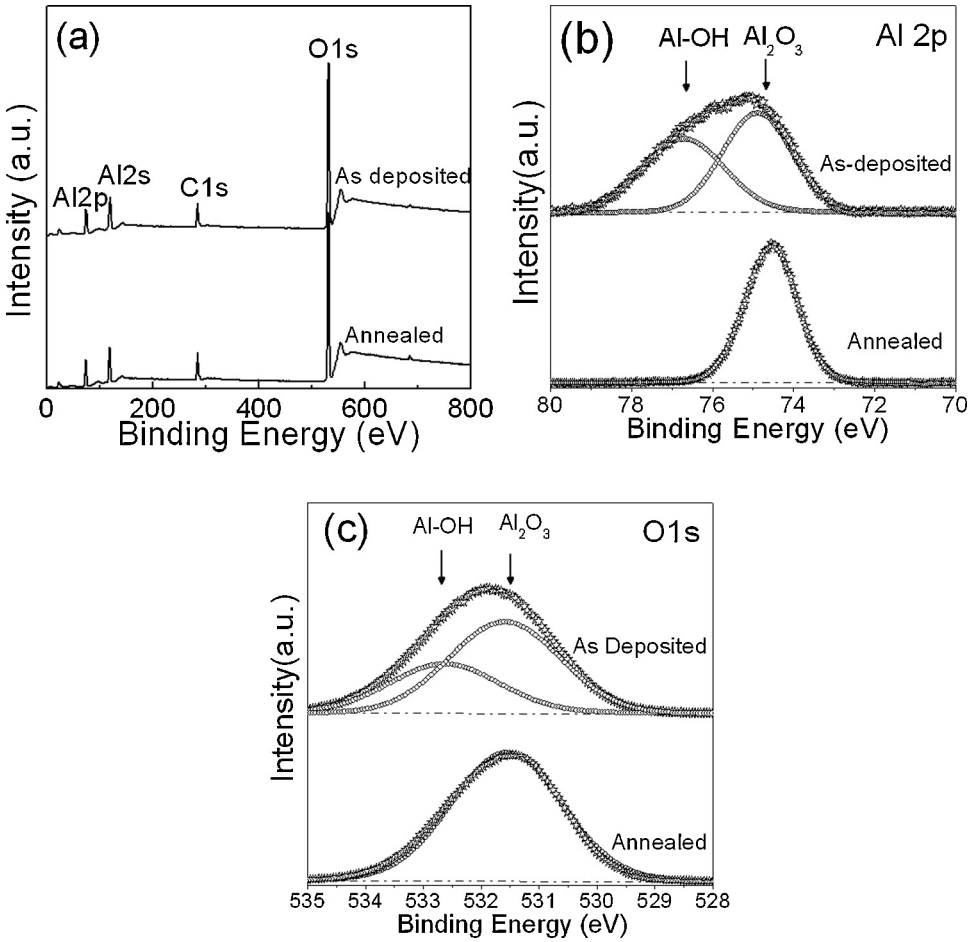

Fig. 5. (a) The wide-survey scan X-ray photoelectron spectra. (b) Al_{2p} core-level XPS spectra. (c) O_{1s} core-level XPS spectra from as-deposited and 550 °C annealed Al_2O_3 films.

helps to the formation of high densities of negative fixed charges within Al_2O_3 films [20]. PDA annealing results in high densities of negative fixed charges in the order of $\sim 10^{12}/cm^2$ within Al_2O_3 films [21]. Such negative fixed charges provide a strong field-effect passivation and high effective minority carrier lifetime (τ_{eff}) [22].

4. Conclusions

In summary, Al_2O_3 layers were deposited by atomic layer deposition on n-type c-Si wafers. Surface anti-reflectance and passivation performances were studied. Average reflectance between 2.8 and 4.2% was obtained for Al_2O_3 coated textured Si with Al_2O_3 thickness ranged between 100 and 70 nm. Passivation performances were also investigated for 100 nm Al_2O_3 coated n-type c-Si wafers. A high minor carrier lifetime of ~4.5 ms is obtained, corresponding to an effective surface recombination velocity of ~4 cm/s. Wide annealing time window and wide annealing temperature window are addressed for obtaining good passivation performances with minor carrier lifetime >3 ms. Such passivation performances were related to the released H atoms from Al–OH bonds and the formation of Al vacancies and O interstitials in Al_2O_3 films. Our results indicate that Al_2O_3 have dual functions of anti-reflectance and surface passivation for potential photovoltaic applications.

Acknowledgements

Programs supported by National Natural Science Foundation of China (11104288) and Zhejiang Postdoctoral Science Foundation (Bsh1202034).

References

[1] M.A. Green, The path to 25% silicon solar cell efficiency: history of silicon cell evolution, Progr. Photovolt.: Res. Appl. 17 (2009) 183–189.
[2] C. Prasittichai, J.T. Hupp, Surface modification of SnO_2 photoelectrodes in dye-sensitized solar cells: significant improvements in photovoltage via Al_2O_3 atomic layer deposition, J. Phys. Chem. Lett. 1 (2010) 1611–1615.
[3] W.W. Hsu, J.Y. Chen, T.H. Cheng, S.C. Lu, W.S. Ho, Y.Y. Chen, Y.J. Chien, C.W. Liu, Surface passivation of Cu(In Ga)Se_2 using atomic layer deposited Al_2O_3, Appl. Phys. Lett. 100 (2012) 023508.
[4] B. Hoex, J. Schmidt, P. Pohl, M.C.M. van de Sanden, W.M.M. Kessels, Silicon surface passivation by atomic layer deposited Al_2O_3, J. Appl. Phys. 104 (2008) 044903.
[5] B. Hoex, M.C.M. van de Sanden, J. Schmidt, R. Brendel, W.M.M. Kessels, Surface passivation of phosphorus-diffused n^+-type emitters by plasma-assisted atomic-layer deposited Al_2O_3, Phys. Status Solidi RRL 6 (2012) 4–6.
[6] H. Lee, T. Tachibana, N. Ikeno, H. Hashiguchi, K. Arafune, H. Yoshida, S. Satoh, T. Chikyow, A. Ogura, Interface engineering for the passivation of c-Si with O3-based atomic layer deposited AlO_x for solar cell application, Appl. Phys. Lett. 100 (2012) 143901.
[7] F. Werner, B. Veith, V. Tiba, P. Poodt, F. Roozeboom, R. Brendel, J. Schmidt, Very low surface recombination velocities on p- and n-type c-Si by ultrafast spatial atomic layer deposition of aluminum oxide, Appl. Phys. Lett. 97 (2010) 162103.
[8] B. Hoex, J. Schmidt, R. Bock, P.P. Altermatt, M.C.M. van de Sanden, W.M.M. Kessels, Excellent passivation of highly doped p-type Si surfaces by the negative-charge-dielectric Al_2O_3, Appl. Phys. Lett. 91 (2007) 112107.
[9] J. Schmidt, A. Merkle, R. Brendel, B. Hoex, M.C.M. van de Sanden, W.M.M. Kessels, Surface passivation of high-efficiency silicon solar cells by atomic-layer-deposited Al_2O_3, Prog. Photovolt.: Res. Appl. 16 (2008) 461–466.
[10] P. Saint-Cast, J. Benick, D. Kania, L. Weiss, M. Hofmann, J. Rentsch, R. Preu, S.W. Glunz, High-efficiency c-Si solar cells passivated with ALD and PECVD aluminum oxide, IEEE Electron Dev. Lett. 31 (2010) 695–697.
[11] J. Benick, B. Hoex, M.C.M. van de Sanden, W.M.M. Kessels, O. Schultz, S.W. Glunz, High efficiency n-type Si solar cells on Al2O3-passivated boron emitters, Appl. Phys. Lett. 92 (2008) 253504.
[12] L.Q. Zhu, J. Gong, J. Huang, P. She, M.L. Zeng, L. Li, M.Z. Dai, Q. Wan, Improving the efficiency of crystalline silicon solar cells by an intersected selective laser doping, Sol. Energy Mater. Sol. Cells 95 (2011) 3347–3351.
[13] P. Saint-Cast, D. Kania, M. Hofmann, J. Benick, J. Rentsch, R. Preu, very low surface recombination velocity on p-type c-Si by high-rate plasma-deposited aluminum oxide, Appl. Phys. Lett. 95 (2009) 151502.
[14] L.A. Dobrzanski, M. Szindler, Al_2O_3 antireflection coatings for silicon solar cells, J. Achiev. Mater. Mfg. Eng. 59 (2013) 13–19.
[15] P. Poodt, A. Lankhorst, F. Roozeboom, K. Spee, D. Maas, A. Vermeer, High-speed spatial atomic-layer deposition of aluminum oxide layers for solar cell passivation, Adv. Mater. 22 (2010) 3564–3567.
[16] H. Park, S. Kwon, J.S. Lee, H.J. Lim, S. Yoon, D. Kim, Improvement on surface texturing of single crystalline silicon for solar cells by saw-damage etching using an acidic solution, Sol. Energy Mater. Sol. Cells 93 (2009) 1773–1778.
[17] L.Q. Zhu, Q. Fang, X.J. Wang, J.P. Zhang, M. Liu, G. He, L.D. Zhang, Structural, optical properties and band gap alignments of ZrO_xN_y thin films on Si (100) by radio frequency sputtering at different deposition temperatures, Appl.Surf.Sci. 254 (2008) 5439–5444.
[18] L.Q. Zhu, Q. Fang, G. He, M. Liu, L.D. Zhang, Microstructure and optical properties of ultra-thin zirconia films prepared by nitrogen-assisted reactive magnetron sputtering, Nanotechnology 16 (2005) 2865–2869.
[19] P.W. Peacock, J. Robertson, Behavior of hydrogen in high dielectric constant oxide gate insulators, Appl. Phys. Lett. 83 (2003) 2025–2027.
[20] K. Matsunaga, T. Tanaka, T. Yamamoto, Y. Ikuhara, First-principles calculations of intrinsic defects in Al_2O_3, Phys. Rev. B 68 (2003) 085110.
[21] L.Q. Zhu, X. Li, Z.H. Yan, H.L. Zhang, Q. Wan, Dual function of antireflectance and surface passivation of atomic-layer-deposited Al_2O_3 films, IEEE Electron Dev. Lett. 33 (2012) 1753–1755.
[22] B. Hoex, J.J.H. Gielis, M.C.M. van de Sanden, W.M.M. Kessels, On the c-Si surface passivation mechanism by the negative-charge-dielectric Al_2O_3, J. Appl. Phys. 104 (2008) 113703.